Phase transitions and optically induced phenomena in cooperative systems

Fausti, Daniele

Publication date:
2008

Link to publication in University of Groningen/UMCG research database

Chapter 1

Introduction and Theoretical Prologue

1.1 Memories and invitation

When I was a child, I was extremely fascinated by the snow melting in the sun. At that time, I would have never thought that this memory could be the starting sentence of my PhD dissertation. Back then, I could not explain to myself how substances made of the same element could display such different properties. Water was liquid and transparent, snow soft and opaque and ice again transparent but extremely hard. Today the title of this dissertation "Phase transitions and optically induced phenomena in cooperative systems" could be reformulated less scientifically but funnier as "The snow melting in the sun, as I see it now".

In thermodynamics a phase transition is the passage of a thermodynamic system from one phase to another without changing its chemical composition. The physical properties of the two phases can be substantially different, and hence the transition can be seen as a sudden (or smooth) change in the physical properties of the system. The most intuitive perspective on how a phase transition can dramatically changes the physical properties of a system comes from those involving a transition of the aggregation state (e.g. solid-liquid, liquid-gas or solid-gas transitions). The best known example of such a transition is probably the water-ice transformation, which obviously changes the mechanical properties of H_2O in a dramatic way. Possibly more difficult to grasp, but no less interesting, are solid-solid phase transitions that do not change the aggregation state of a material but only some of its physical properties like conductivity, stiffness, density, or magnetization. An example of such a phase transition involves the well-known magnetic properties of iron crystals. Due to a transition from a "magnetic" to a "non-magnetic" phase, the attraction between two pieces of iron disappears if the crystal is heated above 750°C, while the solid aggregation changes remains up to

$1300°$C.

The interaction of light with matter lies at the very core of our knowledge of the world. The "optical" investigation of nature started with humankind. It is hard to imagine the amount of "scientific" questions that a sunset, a rainbow, an eclipse or just the properties of a fluorite crystal must have raised in our ancestors. Probably our ancestors, as many of our contemporary fellows, did not pay too much attention to the fact that our vision itself is based on the light-matter interaction. In our eyes, harvesting the electromagnetic bath we happen to live in is the starting point of a process that finally leads to the image of the objects which we form in our brain. In this sense, the interaction of light with matter is one of the most valuable tools that we have to explore and understand the properties of the nature surrounding us. Obviously, in the course of the scientific history of the last centuries, many other investigation tools have been developed. Nevertheless it is interesting to note that the large majority of these "tools" is still substantially based on different kinds of radiation-matter interaction phenomena. The most obvious examples are found in the large variety of spectroscopic techniques available, from γ-rays to the far infrared spectroscopy, which are all based on the interaction between radiation and matter.

On the other hand, it is clear from various examples in nature, that light, apart from being used as an analysis tool, can also strongly affect the properties of matter itself. It can trigger various physical phenomena and can even be used to control matter's behavior and properties. The first intuitive example of a light-induced phenomenon has already been mentioned in the first sentence of this dissertation: heating. When matter absorbs light, the energy carried by the electromagnetic field is taken up by the material and heat is generated. As a consequence of this, the state of matter can be influenced. Returning to the example from my youth, the snow-water phase transition is a marvelous example of *optically induced phase transition.* The energy carried by the sun beams is transformed into thermal energy (vibrations) in the ice and these vibrations, above a certain excitation density, are strong enough to break the bonds between the water molecules inducing melting of the snow crystals. In addition to the optically induced phenomena due to radiation heating, light can transform matter in a way "directly related" to the absorption process itself, and not mediated by the average induced heat. Here one can think of photosynthesis, the vital energy harvesting process in plants, which transforms carbon dioxide and water into glucose and oxygen by making use of the "direct" absorption of light in a receptor molecule and leaving the temperature of the system virtually unchanged (no thermalization process is required).

The knowledge of how the light can perturb a system to the extent that its macroscopical physical properties are changed cannot proceed without understanding the dynamics of the photon-atom interactions. How does the radiation absorption interfere with the material's properties? When are these properties effectively perturbed? How long does the system need to recover equilibrium? These are all questions that on one hand help to understand the phenomena, and

on the other hand point the way to control the properties of matter, out of the thermodynamical equilibrium, using optical techniques. The possibility of shaping the state of a material through irradiation and thereby obtaining transient "phases", i.e. phases with properties not achievable under thermal equilibrium, has stimulated an enormous interest in the scientific community over the last decade. Another aspect that makes this branch of physics extremely appealing is the fact that the laser technology developed over the last two/three decades allows to easily produce extremely short light pulses (less than 10^{-13} seconds). This kindles the hope of controlling those transient properties on extremely short timescales, paving the way to countless potential applications in different fields, from fast electronics to micromechanics. Nowadays it is only possible to speculate on the impact that the ultrafast optical control of material properties will have in the years to come, but given all the recent advances in this field I dear to say: "the future looks bright!"

When a quantum of light - a photon- interacts with matter, many possible processes can happen: absorption, diffusion, scattering. In particular, the research reported in this thesis focuses on a technique based on the inelastic scattering of light, called Raman spectroscopy. When a beam of light interacts with a material, a tiny fraction of the photons (10^{-8}-10^{-10} with respect to the incident ones) are scattered into photon with a different energy. From the study of the characteristic energy of the scattered light, it is possible to retrieve the characteristic excitations of a system and thereby to extract detailed information on its state and symmetry.

It is worth to spend here a few words to explain why Raman spectroscopy is a unique tool for studying photo-induced dynamics and non-thermal phenomena. There are two main Raman scattering processes. In the first one, called Stokes process, the energy of the emitted photons is lower than that of the incoming photons and therefore the system is left in an excited state after the scattering process. Conversely, in scattering processes of the second type, called Antistokes, the energy of the photon leaving the sample is larger than that of the incoming photons and an excitation is annihilated in the sample. It is easy to understand how the Antistokes processes are strongly dependent on the presence of excitations. For example, in a crystal at 0 K, there will be no excitation present and therefore all the Antistokes scattering processes will be quenched. As will be explained later in this chapter, from a comparison of the Stokes and Antistokes intensities, it is possible to monitor specifically the temperature of the investigated excitations. The properties of complex systems are determined by the interplay between different degrees of freedom: vibrational, magnetic, and electronic. Making use time resolved Raman Spectroscopy it is possible to extract detailed information on the temperatures of these different degrees of freedom and thereby to extract detailed information on the nature of the observed processes. If one can follow at the same time the properties and the temperature of a system, one has a unique tool to study the nature of dynamical processes in matter, and in particular to discriminate between thermal and non-thermal processes. Hence the interest to implement time-resolved Raman spectroscopy, a subject which will be described

in the central part of this thesis.

We are just beginning the exploration of the previously inaccessible universe of systems far from the thermal equilibrium. The possibility of inducing material properties non-existent under equilibrium conditions and of controlling them on an ultrafast time scale discloses a world whose laws, and possible applications, are still mainly unexplored. This makes the spectroscopist job in the twenty first century intriguing and compelling!

1.2   Detailed Summary

The work described in this thesis is divided into two main parts. In the first part (chapters 2 and 3), standard Raman spectroscopy, together with different other techniques, is employed to study the magnetic and structural properties of two different families of crystals: $RFe_3(BO_3)_4$ (R = Gd, Tb, Nd, Y and Er) and TiOX (X = Cl and Br). The second part of the thesis (chapter 4, 5, and 6) is devoted to the description of the dynamical version of the Raman spectroscopy. It starts with a description of the technique itself and the set-ups we developed for time resolved Raman spectroscopy (chapter 4), followed by two examples of how the technique can be employed to study optically induced phase transitions in semimetals (chapter 5) and an organic charge-ordered salt (chapter 6).

The second chapter present a study of the cascade of phase transitions characteristic of the family of crystals called "rare-earth-ferroborates". A structural phase transition at high temperature is followed by two magnetic phase transitions at lower temperature: an antiferromagnetic ordering and a spin-flop transition. Through the study of the vibrational properties (phonons) we could reveal that the structural transition has an unusual "weakly first order character". The order parameter of the phase transition was found to display an unusual behavior intermediate between a first order transition (hysteresis) and a second order transition (soft mode behavior). This anomalous phenomenon is explained in the light of the particular symmetry of the crystal structure of this family of compounds. In addition to this, the analysis of the magnetic excitations revealed the presence of short range magnetic correlations in the paramagnetic phase up to unprecedented high temperatures. This will be discussed in Chapter 2 in terms of the low dimensional structural characteristics of the magnetic system.

In the third chapter we present a symmetry disquisition about the different phases of a class of transition metal oxides, namely titaniumoxihalides (TiOCl and TiOBr). The electronic configuration of the Ti ions ($3d^1$), together with the low-dimensional character of the magnetic interaction, make these systems ideal candidates for a Spin-Peierls transition, previously observed in only one other inorganic compound ($CuGeO_3$). Our Raman study of the phase transition focused on two particularly interesting aspects: i) the low temperature phase transition (Spin-Peierls transition) is preceded at higher temperatures by a second phase transition to an intermediate phase; ii) the Spin-Peierls transition has a first order character in contrast to its conventional theoretical description. In chapter 3 we also explain how by studying the symmetry of the vibrational modes characteristic of the three phases, we managed to suggest the space group of the Spin Peierls phase (later confirmed by an X-ray structure determination). Using the same approach we gave some symmetry arguments to rationalize the anomalous first order character of the Spin Peierls transition.

In the fourth chapter we describe the different experimental setups used in the experiments and the commissioning we did to characterize them. The chapter starts with a description of the continuous wave Raman setup where we review

its specifications. In the second part of the chapter the two approaches used for achieving dynamical Raman information will be detailed. The first approach, used for the experiments in chapter 6, is based on a custom made mechanical chopper and achieves a time resolution of $10\mu sec$ and a frequency resolution of $1cm^{-1}$. The second approach makes use of normal interferometric techniques to achieve a time resolution of a few picoseconds at the cost of the frequency resolution which degrades to 8-10cm^{-1}.

In the fifth chapter we report on the study of the elemental crystals of Bismuth and Antimony. The room temperature thermodynamically stable phase of both materials is characterized by a semimetallic behavior due to a Peierls distortion ("Jones-Peierls mechanism"). Through ultrafast Raman measurements, we unraveled two distinct dynamics following intense laser excitation, one ascribed to a thermal and other one to a non-thermal pathway. We could show how, via optical excitation of electrons into the conduction band, it is possible to control, in a non-thermal way, the crystal distortion by reducing the electronic energy gain responsible for the stabilization of the Peierls distortion. Moreover, for excitation fluences larger than $5mJ/cm^2$, corresponding to 3 excited electrons per atom, a new phonon becomes Raman active. We interpreted this as evidence of an optically induced phase transition to a non-thermal "phase" which will hopefully stimulate future studies to clarify its precise nature.

In the sixth chapter we present a study of the previously discovered optically induced insulator-metal phase transition in the organic crystal $(EDO\text{-}TTF)_2PF_6$. Resistivity measurements on this organic salt show a metal to insulator phase transition when the temperature is lowered below 280 K. The low temperature insulating phase is characterized by a charge order on the EDO-TTF molecules. It has previously been shown that by irradiating the low temperature phase with light pulses at 800nm and an extremely low excitation density (1 photon every 500 molecules), it is possible to induce a transient metallic phase, lasting a few hundred microseconds. This phase was suggested to be the high temperature phase. Our transient Raman measurements give clear indication that the photoinduced phase, although also metallic, could be of a different nature than the high temperature phase.

1.3   Theoretical Prologue

There are many topics touched upon on this thesis and the appreciation of the central part of this work requires a background knowledge of different subjects and techniques, not necessarily *"historically related"*. The aim of this section is to summarize this background in a form useful for reading the core of this thesis. The arguments given are not intended to be complete but rather they are meant as an "informal reminder" of fundamental concepts.

In the first part of this section, we shall review the spectroscopic techniques used, focusing mainly on the theory fundament of Raman spectroscopy. In particular we shall give an introduction on the most important scattering processes that will be encountered in the different parts of this thesis. While reviewing the scattering processes we shall give touch on different excitations in solids, focusing on the magnetic ones. In the second part of this section we shall try to give a taste of the theories behind the intriguing solid state phenomena encountered in low dimensional magnetic systems.

1.3.1   "Technique" Physics

Introduction to the Raman Effect

In 1922, the Indian physicist Chandrasekhara Venkata Raman published his work "Molecular diffraction of light"[17]. This was the first of a series of investigations with his collaborators which ultimately led to his publication in 1928 of "A new radiation"[1], that reported the discovery of the radiation effect which bears his name. This effect had been predicted theoretically in 1923 by Smekal, and was independently discovered by Grigory Landsberg and Leonid Mandelstam in 1928. Raman's paper presented the most exhaustive work and in 1930 he was awarded the Nobel Prize for his work.

When light is impinged on a molecule or from a crystal, most of the photons scatter elastically. However, a small fraction of light (approximately 1 in 10^8 photons, depending on the cross section of the specific compound) may scatter inelastically, thereby changing the photon energy. This process of inelastic scattering of light is termed the Raman effect. A large body of literature focuses on the vibrational Raman effect, namely scattering from vibrational and rotational excitation in molecules and solids. The Raman effect is, however, much more general since it is not limited to the vibrational effect, but also refers to scattering processes from other fundamental excitations. Indeed, inelastic light scattering, such as that from magnetic and electronic excitations, has proven to be a valuable tool in contemporary condensed matter physics. The introductory nature of this section leads us to proceed with the following logic: we shall firstly start with a simple classical model explaining the Raman effect for molecules, in an attempt to make it intuitively clear. Secondly, we shall discuss the effect in crystals and finally treats the quantum mechanical scattering process in more details to ex-

plain the "thermodynamic" information revealed by this technique. This will be useful to clarify the specific potential of Raman spectroscopy for studying non thermal processes. The second part of the chapter is devoted to the introduction of the concept of magnons and of Raman scattering from magnetic excitations. In the final part we shall introduce some peculiarities of low dimensional magnetic systems.

Classical Description   The classical description of Raman scattering interprets the scattering as originating from a change in molecular polarizability due to the presence of vibrational modes in the system. For an applied electromagnetic field $E(\omega)$, the polarizability α_0, gives a dipole moment $P_D(\omega) = \alpha_0 E(\omega)$, which acts as a source of an evanescent wave. If the molecule is vibrating at the frequency of a vibrational eigenmode (Ω), the polarizability becomes modulated at the same frequency by an additional term $\alpha_1 = \frac{d\alpha}{dr}$. We can write the dipole moment as $P_D(\omega) = (\alpha_0 + \alpha_1 \cos(\Omega\, t))E(\omega)$ and by substituting the field with a plane wave, it is easy to obtain:

$$P_D(\omega) = \alpha_0 E_0 cos(\omega\, t) + \alpha_1 E_0/2[cos((\omega + \Omega)t) + cos((\omega - \Omega)t)] \qquad (1.1)$$

Thus the evanescing light oscillates mainly at the field frequencies ω, but also at two frequencies $\omega - \Omega$ (Stokes line) and $\omega + \Omega$ (Antistokes). In normal cases, α_1 is many orders of magnitude smaller than α_0, thus the side bands are extremely weak compared to the elastically scattered light. A vibration will give a Raman response if it induces a change in the molecular polarizability. This is not necessarily the case for any vibration, but rather depends on the particular deformation induced. For the calculation of the molecular selection rule using molecular point group symmetry we refer to [3].

Phonons in solids have a periodic structure and this causes the Raman scattering process to be directional for a given phonon and a given excitation intensity. To put it simply, to evaluate the scattering cross section, it is necessary to take into account the interference between photons scattered in different parts of the crystal. The constructive interference will be given for $sin(\theta/2) = n\lambda/2\Lambda$, where θ is the angle between the incident and scattered light, n the refractive index of the crystal, λ the wavelength of the incident light, and Λ the wavelength of the phonon[1].

To describe the scattering processes in crystals, following the approach of [2], we can proceed in a similar manner, namely by expanding the susceptibility tensor χ_{ij} in terms of the the normal coordinates of the phonons (Q_k) instead of the atomic displacements of Eq.1.1.

$$\chi_{ij} = (\chi_{ij})_0 + \sum_k (\frac{\partial \chi_{ij}}{\partial\, Q_k})Q_k + h.o. \qquad (1.2)$$

---

[1]The usual "almost flat" dispersion of optical phonon close to the k=0 point of the Brillouin zone, will make the directionality of the average signal weak. This is the reason why in most of the experiments, a small misalignment of the crystal axis will not be crucial.

The coefficients $\frac{\partial \chi_{ij}}{\partial Q_k} = \chi_{ij,k}$ constitutes a tensor also known as the Raman tensor, and the intensity of the Raman scattered light is proportional to its square. The induced dipole moment which accounts for the emission of the side bands is (with an incident field $E_l^i(t) = E_{l,0}^i cos(\omega t)$ and the phonon expressed as $Q_k = Q_{k0} cos(\Omega_k t)$):

$$P_{Dj}^s(\omega \pm \Omega_k) = \chi_{jl,k} \varepsilon_0 V_u E_{l0}^i Q_{k0} \cos(\omega \pm \Omega) t \qquad (1.3)$$

where V_u is the volume of the unit cell. The scattering intensity is proportional to the square of the dipole moment, P_D^s, which is given for a mode and for a selected direction of polarization, e^s, of the scattered light by the square of the projection of P_D^s on e^s:

$$\phi(k) = C|e^s P_D^s|^2 = C|\sum_j e_j^s P_{Dj}^s(k)|^2 \qquad (1.4)$$

where P_{Dj}^s are the components of the dipole moment induced by the Raman effect given by Eq.1.3. It follows that the scattering intensity is given by:

$$\phi(k) = C|\sum_{jl} e_j^s \chi_{jl,k} e_l^i|^2 \qquad (1.5)$$

Eq.1.5 shows how it is possible to measure any component of the Raman tensor by selecting the proper combination of the incoming and scattered polarization.

Selection Rules Crystals can be classified in terms of the symmetry operations required to generate all the crystal (with the atoms at the equilibrium positions) starting from a single atom or a basis (for non-primitive lattices). The set of these symmetry operations obeys the mathematical criteria for a group and is called the "Space group". The determination of the number of vibrational modes, their symmetry, and hence the selection rule for infrared and Raman absorption becomes easier when making use of the group theoretical analysis. The scalar properties such as temperature and density of a crystal, will be invariant under the symmetry operation of the group. Conversely, vectorial and tensorial properties like dipole moments and susceptibility, are not invariant under the symmetry operation of the group. Vectorial properties transform like the coordinates (x,y and z), while tensorial properties transform as the products of the cartesian coordinates. Similarly, the symmetry representations for the susceptibility tensor are the same as those of quadratic terms involving the Cartesian coordinates, x^2, y^2, z^2, xy, yz, and xz. That means that an excitation is not infrared-active if its representation does not contain terms transforming as the cartesian coordinates under the symmetry operations of the group. In the same way, excitations involving a change in the susceptibility of the crystal must have the representation of the quadratic form, since excitations without this characteristic will not be Raman active. A particularly interesting case is that of centrosymmetric crystals, where the presence of an inversion center (written as the symmetry operator $x, y, z \longrightarrow -x, -y, -z$) make the infrared and Raman activity mutually exclusive.

Quantum Mechanics A theoretical description of the Raman scattering proceeds by calculating quantum mechanically the dipole moment induced by the incident light; this is done through the second order perturbation theory considering a classical electromagnetic field as a perturbation. By subsequently making use of the "correspondence principle", the intensity of the radiation emitted by the dipole moment is calculated by the classical expression for an oscillating dipole. The full description goes beyond the purpose of this thesis and can be found elsewhere ([7]). The aim here is to give an insight into how thermodynamics come into play, giving access, through the ratio of Stokes to Antistokes intensities, to a local temperature measurement. The schematic view of Raman scattering is sketched in Fig.1.1. In the left part (Stokes process), an electron is excited by a photon and this excitation is followed by a recombination with a simultaneous emission of a photon of different energy. Also in the Antistokes process the final state $(< f|)$ differs from the initial one $(|i >)$ by the absorption of an excitation of the system, and is reached from the initial state via an intermediate state. This could be a real electronic state (resonant Raman scattering) or a virtual one.
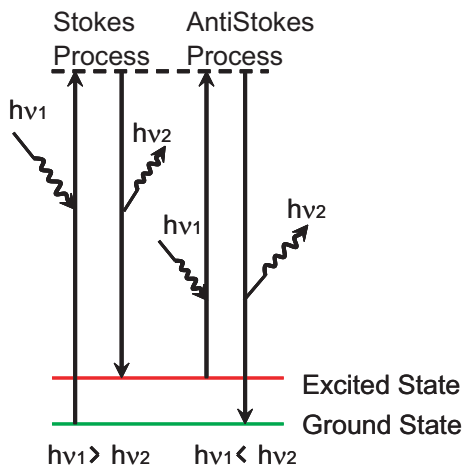

Figure 1.1: *Schematic view of the Raman process. The Stokes process creates an excitation in the system, while the Antistokes annihilates one.*

The quantum mechanical analogue of Eq.1.3, describing the polarization induced by an electromagnetic field is $P_{fi} = < f|\varepsilon_0 \chi \; E|i >$, where $< f|$ and $< i|$ are wave functions considering both electronic and nuclear coordinates. Following the adiabatic (or Born-Oppenheimer approximation) the total wave functions can be factorized in a electronic part $\varphi(x, X)$ and a nuclear part $\varrho(X)$. If the wavelength of the field is larger than the interatomic distances we can extract the field from

the integral and obtain:

$$< f|\chi|i >= \int \varrho_f^*(X)\varphi_f^*(x,X)\chi\varphi_i(x,X)\varrho_i(X)dxdX \qquad (1.6)$$

Considering that only the electronic part of the susceptibility is still dependent on the atomic coordinates, we can expand it in term of the normal coordinates (Q_k):

$$< f|\chi|i >= (\chi)_0 < ..\nu_{fk}..|..\nu_{ik}.. > + \sum_k (\frac{\partial \chi}{\partial Q_k})_0 < ..\nu_{fk}..|Q_k|..\nu_{ik}.. > \quad (1.7)$$

Where the *bra* an *ket* represent the total vibrational wave function of Eq.1.6, and they are expressed as the product of harmonic oscillator wave function, where the ν_{ik} and ν_{fk} are their occupation numbers:

$$< \nu_{f1}..\nu_{fk}..\nu_{fn}| = \prod_k < \nu_{fk}| \quad \text{and} \quad < \nu_{i1}..\nu_{ik}..\nu_{in}| = \prod_k < \nu_{ik}| \qquad (1.8)$$

where $< \nu_{fk}|$ and $< \nu_{ik}|$ again stay for harmonic oscillator wave function with occupation number ν_{fk} and ν_{ik}. The products between two wave function are:

$$< \nu_{fk}|\nu_{ik} >= \begin{cases} 0 , & \text{for } \nu_{fk} \neq \nu_{ik} \\ 1 , & \text{for } \nu_{fk} = \nu_{ik} \end{cases}$$

and the normal coordinate expectation value is:

$$< \nu_{fk}|Q_k|\nu_{ik} >= \begin{cases} 0 , & \text{for } \nu_{fk} = \nu_{ik} \\ (\nu_{ik} + 1)^{1/2}\sqrt{\hbar/2\Omega_k} , & \text{for } \nu_{fk} = \nu_{ik} + 1 \\ (\nu_{ik})^{1/2}\sqrt{\hbar/2\Omega_k} , & \text{for } \nu_{fk} = \nu_{ik} - 1 \end{cases}$$

The first term in Eq.1.7 is different from zero only if $\nu_{fk} = \nu_{ik}$, so that the final state population is unchanged (Rayleigh scattering). The second term, as made clear by the derived susceptibility, describes the Raman scattering. According to Eq.1.9, this term is different from zero for the mode k $\nu_{fk} = \nu_{ik} \pm 1$, where Eq.1.7 is reduced to:

$$< \nu_{ik} + 1|\chi|\nu_{ik} >= (\nu_{ik} + 1)^{1/2}\sqrt{\hbar/2\Omega}(\frac{\partial \chi_{mn}}{\partial Q_k})_0 \qquad (Stokes)$$

$$< \nu_{ik} - 1|\chi|\nu_{ik} >= (\nu_{ik})^{1/2}\sqrt{\hbar/2\Omega}(\frac{\partial \chi_{mn}}{\partial Q_k})_0 \quad (Antistokes)$$

$$(1.9)$$

Comparing these equations with Eq.1.2, one notes the equivalence between the tensor for the transition susceptibility and the derived susceptibility multiplied with the amplitude of the normal coordinates. In the quantum mechanical calculation the amplitude of the normal coordinate is replaced by the quantum mechanical equivalent $\sqrt{\hbar/2\Omega}$. Attention must be paid to the dependence of the

scattering intensity on the occupation number, ν_k, determined by the Boltzmann factor:

$$W(\epsilon_k) = \frac{exp(-\epsilon_k/K_BT)}{Z} = \frac{exp[-\hbar\Omega_k(\nu_k+1/2)/K_BT]}{\sum_{\nu_k} exp[-\hbar\Omega_k(\nu_k+1/2)/K_BT]} \qquad (1.10)$$

and a thermal average of the form $\sum_{\nu_k}(\nu_k+1)W(\epsilon_k)$ is required to obtain the effective square of the tensor in Eq.1.9. Assuming the Raman tensor to be equal for the two processes (reasonable for transparent samples, but not at the edge of an absorption band), it is clear that the intensity of Stokes and Antistokes ratio is dependent on the local temperature on the sample as:

$$\frac{\phi_A}{\phi_S} = (\frac{\omega+\Omega_k}{\omega-\Omega_k})^4 exp(\frac{-\hbar\Omega_k}{K_BT}) \qquad (1.11)$$

The intensities of the second-order Raman lines are obtained from the higher order expansion of the susceptibility and the statistics obtained are summarized in Tab.1.1. These are given in terms of the phonon mean occupation number n_i ($n_i = [exp(-\hbar\omega/k_BT) - 1]^{-1}$), and the intensities of the scattered light are proportional to the square of the result.

Table 1.1:

Process	Stokes	Antistokes
One-Phonon	$1+n_i$	n_i
Two Phonon (Overtones)	$2+3n_i+n_i^2$	$n_i^2-n_i$
Summation	$1+n_i+n_j+n_in_j$	$1+n_i+n_j$
Difference	$n_j+n_in_j$	$n_i+n_in_j$

This gives an extremely useful insight on the possible application of Raman spectroscopy in dynamical studies of matter.

Provided that the matrix elements of stokes and antistokes scattering don't change in time, Raman spectroscopy provides a local probe for the temperature of the excitation under investigation, potentially allowing us to disentangle in a single measurement the real time evolution of, for example, electron, spin and lattice temperatures.

Raman Scattering from Magnetic Excitations

The experimental report of inelastic light scattering processes from magnetic excitation is almost 40 years younger than Raman's observation of the vibrational ones. The first observation of Raman scattering from magnetic excitations was only reported in 1966 for the antiferromagnet FeF_2[11]. The presence of magnons in magnetic materials causes a periodic modulation of the material's permittivity and light is scattered by this permittivity fluctuation.[8] A direct coupling between spin fluctuation and magnetic vector was shown to be negligible respect to

the first process.[8] To illustrate the light scattering process in a magnetic system, we follow the approach of reference [6].

The incident electric field E_I^i will produce a polarization proportional to the susceptibility $P^j(r,t) = \epsilon_0 \sum_i \chi^{ji}(r,t) E_I^i(r,t)$, where i and j indicate the three cartesian coordinates, ϵ_0 the free space permittivity, and χji the susceptibility tensor. As described in the previous section, the polarization acts as the source of the scattered field and the evaluation of the scattering cross section will be reduced to the evaluation of the correlation function $< \chi^{\alpha\beta} \chi^{\mu\nu} >_\omega$ (where the $\alpha, \beta, \mu,$ and ν indicate the cartesian coordinates). The effective Hamiltonian describing the interaction of light with a magnetic system can be regarded as the electric dipole interaction between the polarization vector and the scattered field in a particular direction, E_S^j: $H = \sum_r \sum_{i,j} E_S^i \chi^{ij}(r) E_I^j$, where the sum over r indicates the sum over different magnetic sites. In magnetic materials the susceptibility can be a spin dependent quantity, and using a similar approach to the one previously described for vibrational Raman spectroscopy, we can expand the susceptibility at the site r in terms of the spins operators:

$$\chi^{ij}(r) = \chi_0^{ij}(r) + \sum_\mu K_{ij\mu}(r) S_r^{mu} + \sum_{\mu,\nu} G_{ij\mu\nu} S_r^\mu S_r^\nu +$$
$$\sum_\delta \sum_{\mu,\nu} H_{ij\mu\nu}(r,\delta) S_r^\mu S_{r+\delta}^\nu + h.o. \qquad (1.12)$$

The first term, χ_0^{ij}, is the susceptibility in the absence of magnetic excitation and will give rise to elastic scattering.

The one magnon scattering processes can be mostly described by the next terms (K and G), involving the spin operator on a single site. The linear coupling coefficient, K, is proportional to the magnetic circular birefringence, while the quadratic term, G, is proportional to the magnetic linear birefringence. The main macroscopic mechanism for the one magnon scattering process goes through electric dipole coupling of radiation to the crystal and relies on the spin-orbit coupling ($\lambda L \cdot S$) in the electronic excited state for changing the ion spin state. Further insight into the so-called Elliot-Loudon mechanism can be found elsewhere ([6, 18]). This thesis mostly concerns antiferromagnetic systems, where the main scattering process is the two magnon scattering, described by the last term of Eq.1.12 (H) and involving a pair of spin operators on different sites. This term can provide an additional (small) contribution to one magnon scattering, but what is more interesting, is that the term involving the H tensor gives rise to two magnon scattering, in which a pair of magnons is created or destroyed. In the Stokes process the frequency shift of the incoming light will be the sum of the frequencies of the two magnons created, $\Delta\omega = \omega(q) + \omega(q')$. Since the momentum of light, k, is very small with respect to the Brillouin zone, the momentum conservation law gives $q \approx -q'$ (see Fig.1.2 (a)). It appears straightforward that the two magnon processes are not limited (as the one magnon scattering) to the center of the Brillouin zone. Indeed, the two-magnon scattering feature results in a peak

near the frequency region where the magnon excitation spectra have the highest
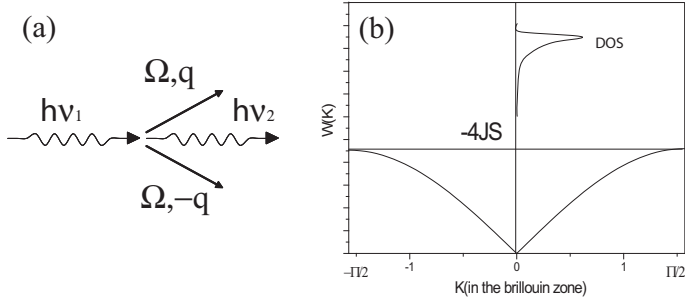density of states, and this usually happens at the zone boundary (Fig.1.2(b)).

Figure 1.2: *Schematic view of the two magnon Raman scattering for antiferromag-
netic samples. (a) In the scattering process, two magnons with opposite wave vector are
created. To make the example clear, a sinusoidal magnon dispersion, derived for a one
dimensional antiferromagnet, has been depicted (b). The two magnon scattering feature
is proportional to the density of state of the magnon dispersion.*

The Elliot-Loudon process will give a contribution when extended to a higher
order. However, this mechanism predicts a cross section substantially smaller
than that of the one-magnon process. Conversely, as anticipated, experiments
on antiferromagnets revealed that the two magnon scattering is of comparable
intensity (and larger) than the one-magnon feature. This inconsistency was re-
solved by a suggestion of an alternative and more efficient scattering process for
antiferromagnet, called the exchange-scattering mechanism[12].

We shall now try to give a simple explanation of the two magnon scattering
processes in an antiferromagnet. The magnon excitation spectrum in a simple
antiferromagnet consists of two magnon branches, corresponding to the spins
precessing in opposite directions on the two sublattices $\omega^{\pm}(k)$. Physically the
two branches correspond to excitations in which the total S^z operator changes by
1. It is easy to show that the two branches became degenerate in the case of 0
applied magnetic field [6]. The function which describes the state of each branch
is denoted with $|k, +>$ and $|k, ->$ to indicate whether the S^z is increased $(+)$
or decreased $(-)$. The linearly independent two-magnon state with wave vector
k and $-k$ can be constructed as follows:

$$
\begin{aligned}
&|a> = |k, +>|-k, +> & \Delta S^z = +2 \\
&|b> = 2^{-1/2}[|k, +>|-k, -> +|k, ->|-k, +>] & \Delta S^z = 0 \\
&|c> = 2^{-1/2}[|k, +>|-k, -> -|k, ->|-k, +>] & \Delta S^z = 0 \\
&|d> = |k, ->|-k, -> & \Delta S^z = -2
\end{aligned}
\tag{1.13}
$$

The states $|a>$ and $|d>$ with $\Delta\,S^z = \pm 2$ correspond to the one-magnon processes extended to higher order (the state $|d>$ is the only two-magnon state possible in a ferromagnet where the excitation spectrum is "single-branched"). The $|b>$ and $|c>$ terms ($\Delta\,S^z = 0$) describe spin deviations created on opposite magnetic sublattices, on sites which are exchange-coupled through a virtual electronic transition to higher states. The state with even parity ($|b>$) corresponds to two-magnon scattering processes, while the one with odd parity ($|c>$) is more relevant for two-magnon absorption processes. This results in a much more efficient scattering process than the one described as the one-magnon scattering extended to higher order. Moreover, this shows that two-magnon scattering arises mainly from a physically different process, and hence there is no a priori reason to expect the two-magnon intensity to be weaker than the one-magnon feature in antiferromagnets.

Time Resolved Reflectivity

Another technique which in the framework of the research of this thesis was used in the experiments described in chapter 5 and 6 is Time-Resolved-Reflectivity (TRR). Widely employed in the last 20 years thanks also to the availability of cheap ultrafast laser sources, TRR was probably the first basic experiment to study ultrafast dynamics in solids (even though often not the "more straightforward" to interpret). To give just a taste of the information available from a transient reflectance experiment, it is necessary to understand where the reflectivity changes induced by light irradiation come from. To give a simple introduction to this huge family of experiments, we follow the approach suggested by Zieger[4]. If R is the unperturbed reflectance, the fractional changes of reflectance after irradiation can be written: $\frac{\Delta R(t)}{R} = \frac{1}{R}\left(\frac{dR}{dn}n(t) + \frac{dR}{dT_E}\Delta T_E(t) + \frac{dR}{dQ}Q(t) + \frac{dR}{dT_l}\Delta T_l(t)\right)$. Here the first term accounts for the electron excited in the conduction band, the second one for the changes in the electronic temperature, the third for the lattice displacement[2], and the fourth for the variation in lattice temperature[3]. The timescales for the electronic and lattice thermalization are expected to be different and, as will be seen in chapter 5, this will allow us to distinguish between the two. Nevertheless, it must be made clear that disentangling the different contributions is not always easy, and usually requires a model based on a series of assumptions suitable for describing the physics of the investigated system.

---

[2]This term is generally used to describe the "Coherent Phonon excitation". The 'sudden' displacement of the atoms from their equilibrium position (through different suggested mechanisms, DECP[4], ISRS[16], or others[9]) will force the atoms to oscillate in phase around the equilibrium position, which would modulate the reflectivity with the frequency of the vibrational eigenmode.

[3]The last term is not present in Zeiger approach and it has been added for clarity

1.3.2 "Material" Physics

Low Dimensional Magnetic Systems

The understanding of low dimensional magnetic systems is a topic of major interest for the condensed matter physicist in the last years. The effect of the reduced dimensionality on magnetic systems gives life to a novel branch of physics, whose properties, dominated by quantum fluctuation and non-thermal disorder, are far from being completely understood. The theoretical bottom line to study the low dimensional system is the Mermin-Wagner theorem. It states that continuous symmetries cannot be spontaneously broken at a finite temperature in one and two dimensions. This is because if such a spontaneous symmetry breaking occurred, then the corresponding Goldstone bosons, being massless, would have an infrared divergent correlation function. Intuitively, this means that long-range fluctuations can be created with little energy cost and since they increase the entropy they are favored, and therefore they would destroy the order. As an example, Heisenberg spin systems, where the interaction Hamiltonian is $S_i \cdot S_j$, the field excitations are called spin waves and can be recognized as Goldstone bosons. The excitation spectra of spin waves is gapless. It can be shown that for these excitations spectra fluctuations would destroy the order in 1 dimension and would allow a 2 dimensional order only at T=0. On the other hand the three dimensional order would be allowed. A formal description of the Mermin-Wagner theorem goes beyond the purpose of this introduction and can be found elsewhere[9].

The central part of chapter two (and partially chapter three) deals with magnetic systems where the interactions are of quasi-one-dimensional nature. As for this introduction, the aim is simply to point out how fluctuations can play a key role in determining the properties of quasi-one/two-dimensional systems.

Landau theory of phase transitions

It is worth including in the theoretical prerequisites of this thesis a short introduction to the Landau theory of phase transitions. In chapter 2 we shall make use of the Landau theory to together with some symmetry arguments to explain the first order character of the temperature induced structural phase transition in the borates family. We shall also rely on the Landau theory of phase transitions in Chapter 5 to discuss phonon screening by an excited electron/hole plasma. The phonon softening observed will be proposed as a precursor of an optically induced phase transformation and discussed in the spirit of the Landau theory.

The Landau theory assumes that the free energy of a system is determined by some parameters called the order parameters, and can be expressed analytically in terms of the order parameters. The choice of the order parameters depends on the physics of the investigated system. As an example, in the cases investigated in chapter 2 and 5, the order parameter will be the distortion of the lattice[4]. Note

---

[4]The description of the dynamical distortion in chapter 5 will make use of two coupled order

that in spite of the different nature of the phenomena investigated in chapter 2 and in chapter 5, the description in terms of the Landau theory is "relatively" similar.
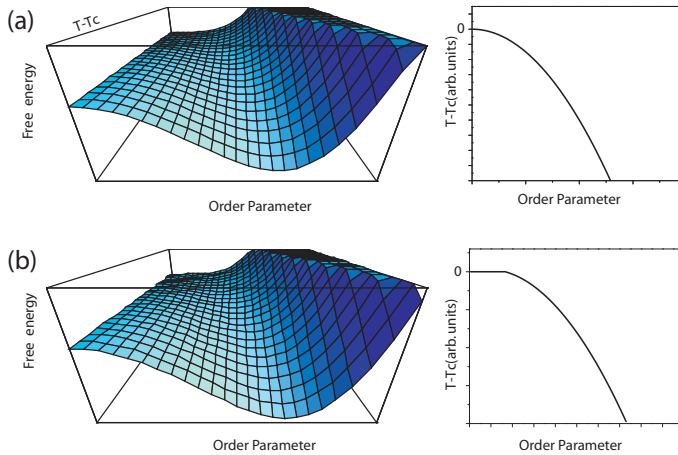

Figure 1.3: *Free energy in the Landau description, considering all the terms (b) and only the even ones (a). On the right a plot of the order parameter as a function of temperature is depicted for the two cases.*

At a finite temperature, the order parameter will have a certain value (ϵ_0) that minimizes the free energy, so that $F(\epsilon_0, T) \leq F(\epsilon, T)$ for any other $\epsilon \neq \epsilon_0$[5]. The appearance of a minimum of the free energy for different values of ϵ at different temperatures describes the system approaching a phase transition. The free energy of the system obeys two main requirements: it is analytic and it satisfies the symmetry requirements of the Hamiltonian. In the vicinity of the equilibrium position the free energy $F(\epsilon, T)$ can be expanded in power terms of the order parameter: $F(\epsilon, T) = q_0 + q_1\epsilon^2 + q_2\epsilon^3 + q_3\epsilon^4 + h.o.$ [6].

In general, all the expansion coefficients have to be taken into account but the symmetry requirements of the specific investigated problem can help in simplifying the description. The most common simplification is the case of a centrosymmetric Hamiltonian, where all the odd terms of the expansion vanish due

---

parameters, the distortion of the lattice and the number of electrons excited in the conduction band.

[5]The free energy should also contain an entropy term ($-TS(\epsilon, T)$), but for simplicity we assume that this term is constant at all ϵ - ie. this corresponds to the assumption that the volume and the number of particles are constant at different ϵ.

[6]The first term of the expansion is neglected due to the fact that ϵ_0 is an equilibrium position: $\frac{dF}{d\epsilon}(\epsilon_0) = 0$.

to symmetry reasons. In this case it is common to express the first term in the free energy's expansion as changing sign at the phase transition: $q_1 = a(T - T_0)$. Hence, the free energy minimum (the order parameter) approaches 0 continuously (Fig.1.3(a)), describing a second order phase transition. If the symmetry of the Hamiltonian allows the even terms of the expansion to be non-zero (as an example, see Appendix A, Chapter 2) the situation changes. The order parameter shows a discontinuity at T_c, as typical for 1st-order phase transitions, and subsequently shifts as in 2nd-order phase transitions (Fig.1.3(b)). This will be used in Chapter 2 to describe a "weak first-order" phase transition.

Magnons

A full description of magnetic excitations goes beyond the purpose of this thesis. Nevertheless, a general introduction on spin waves and magnetic excitation is necessary to understand the following chapters of this thesis and has therefore been included below.

As for lattice vibrations, where the notion of phonons as quantized lattice excitation has been introduced, a magnon is the quantized excitation of the magnetic system (the classical analogue is a spin wave). The simplest way to understand and visualize spin waves is to consider the Heisenberg Hamiltonian $H = -J \sum_{i,j} S_i \cdot S_j$. For $J > 0$ the energy is minimized when the spins on different atoms are oriented parallel to each other, with a total magnetic energy gain of $U = NJS^2$. Hence, as sketched in Fig.1.4(a), the ground state for $J > 0$ will be ferromagnetic ($|... \uparrow\uparrow\uparrow ... >$). Similarly it can be seen that $J < 0$ will give rise to an antiferromagnetic ordering ($|... \uparrow\downarrow\uparrow\downarrow ... >$, Fig.1.4(b)). In general the situation can be more complex: the anisotropy can be of a different nature and long range interaction can be relevant. In addition, in solids with different atomic species, multiple interactions are usually present, and in some cases an interaction can be even "frustrated", a term used to indicate that different interactions cannot be satisfied simultaneously. Therefore, it is natural to expect that a variety of different ground states could appear, ranging from canted antiferromagnet to sinusoidal order or spiral ordered states.

To introduce the spin wave calculation, we consider the ideal case of a one dimensional antiferromagnet sketched in Fig.1.4(a). The excitation spectra and the dispersion relations of an Heisenberg Hamiltonian, in the approach of [13, 14], are calculated starting from the equations of motion for the spin S_i at the site i. Assuming that the spins are aligned ($S_z = S$) and that $S_x, S_y << S_z$, the equation of motion for S_z is of second order in S_x, S_y and can be neglected. By transforming the equation of motion into the momentum, space it is possible to show that in the excited states the spins precess along the z-axis with the same frequency but different phase (Figure 1.4(c)). For an antiferromagnet, the situation is similar and the simultaneous treatment of the two magnetic sublattices is needed ($\uparrow$ and
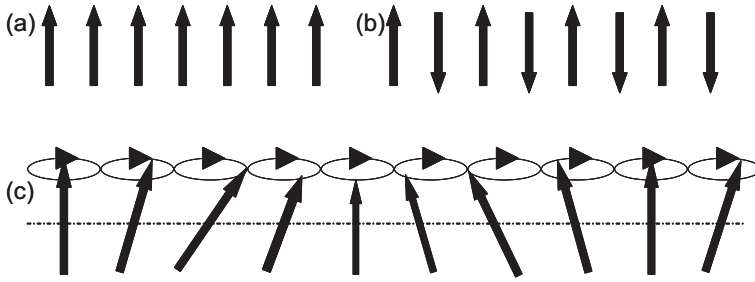
Figure 1.4: *Sketch of a ferromagnetic (a) and antiferromagnetic order (b). (c) Sketch of a spin wave excitation for a one dimensional ferromagnetic system.*

$\downarrow$). It can be shown that the main difference is the appearance of an optical branch in the excitation spectra [4]. Further details on the spin wave calculation can be found elsewhere [19].

1.3.3 Summary

To summarize, the aim of this chapter was to help make the rest of this work more readable. We tried to put together a summary of background knowledge on different subjects in a simple and useful way for further reading. In the first part we gave a general motivation for this study, and a short introduction to every chapter. In the second half, we gave an overview of the theoretical foundation of the experimental techniques used and, at the same time, we tried to give the "flavor" of some of the problems investigated.

Bibliography

[1] V. Raman, Indian J. Phys. **2**, 387 (1938).

[2] H. Kuzmany, *Solid-State Spectroscopy* (Springer, Berlin, 1998).

[3] P. Atkins' and J. de Paula, *Physical Chemistry* (Oxford university press, Oxford, 2006).

[4] C. Kittel, *Introduction to Solid State Physisc* (John Wiley & Sons, New York, 1996).

[5] D. Komskii, *Quantum Solid State - Course Notes* .

[6] M. G. Cottam and D. J. Lockwood, *Light Scattering in Magnetic Solids* (JohnWilley & Sons, New York, 1986).

[7] P. Brüesch, *Light Scattering in Magnetic Solids* (JohnWilley & Sons, New York, 1986).

[8] R. Loudon, Proceedings of the Royal Society of London. Series A, Mathematical and Physical Sciences **275**, 218 (1963).

[9] N. D. Mermin, H. Wagner, Phys. Rev. Lett. **17**, 1133 (1966).

[10] R. Loudon, Advances in Physics **50**, 813-864 (2001).

[11] P. A. Fleury, S. P. S. Porto, L. E. Cheesman, H. J. Guggenheim, Phys. Rev. Lett. **17**, 84 (1966).

[12] P. A. Fleury, S. P. S. Porto, R. Loudon, Phys. Rev. Lett. **18**, 658 (1967).

[13] T. Holstein, H. Primakoff, Phys. Rev. **58**, 1098 (1940).

[14] F. Bloch, Z. Physik **61**, 206 (1930).

[15] D. M. Sagar, A. A. Tsvetkov, D. Fausti, S. van Smaalen, P. H. M. van Loosdrecht, JOURNAL OF PHYSICS - CONDENSED MATTER **19**, 346208 (2007).

[16] G. C. Cho, W. Kutt, H. Kurz, Phys. Rev. Lett. **65**, 764 (1990).

[17] C. V. Raman, *On the Molecular Scattering of Light in Water and the Colour of the Sea* (Proceedings of the Royal Society, 1922).

[18] W. Hayes and R. Loudon, *Scattering of light by crystals* (JohnWilley & Sons, New York, 1978).

[19] put toghether by A. Zheludev (2006), "http://neutron.ornl.gov/ zhe-lud/useful/dispforweb/index.html".